

Eclipsing Binaries in the OGLE Variable Star Catalog. IV. The Pre-Contact, Equal-Mass Systems

CARLA MACERONI

Electronic-mail: *maceroni@coma.mporzio.astro.it*

Rome Observatory, via Frascati 33, I-00040 Monteporzio C., Italy

and

SLAVEK M. RUCINSKI

Electronic-mail: *rucinski@astro.utoronto.ca*

David Dunlap Observatory, University of Toronto
P.O.Box 360, Richmond Hill, Ontario, Canada L4C 4Y6

September 9, 2017

ABSTRACT

We used the database of eclipsing binaries detected by the OGLE microlensing project in the pencil-beam search volume toward Baade's Window to define a sample of 74 detached, equal-mass, main-sequence binary stars with short orbital periods in the range $0.19 < P < 8$ days. The logarithmic slope of the period distribution, $\log N \propto (-0.8 \pm 0.2) \log P$, was used to infer the angular-momentum-loss (AML) efficiency for the late, rapidly-rotating members of close binaries. It is very likely that the main cause of the negative slope is a discovery selection bias that progressively increases with the orbital period length. Assuming a power-law dependence for the correction for the bias $\propto -C \log P$ (with $C \geq 0$) the AML braking-efficiency exponent α in $dH/dt = P^{-\alpha}$ can take any value $\alpha = -1.1(\pm 0.2) + C$. Very simple considerations of discovery biases suggest $C \simeq 4/3$, which would give an AML braking law very close to the "saturated" one, with no dependence on the period. However, except for plausibility arguments, we have no firm data to support this estimate of C , so that α remains poorly constrained. The results signal the utmost importance of the detection bias evaluation for variable star databases used in analyses similar to the one presented in this study.

Subject headings: binaries: close — binaries: eclipsing — stars: late-type — stars: rotation

1. INTRODUCTION

This paper is a continuation of the analysis of the eclipsing binaries detected by the OGLE microlensing project in the nine central fields of Baade's Window (BWC to BW8) toward the Galactic Bulge (Udalski et al. 1994, 1995a, 1995b). The three previous papers of this series addressed the properties of contact binaries which are the most common type in the sample of 933 eclipsing systems in Baade's Window (BW). The first paper (Rucinski 1997a = R97a) showed that – due to their high frequency of incidence – the contact systems of the W UMa-type can be useful distance indicators along the line of sight all the way to the Galactic Bulge and that they belong to the old galactic disk population. The second paper (Rucinski 1997b = R97b) discussed the light curves of those systems. The light-curve amplitude distribution strongly suggested a mass-ratio distribution steeply climbing toward low mass-ratios (i.e. unequal masses). The systems with unequal temperatures of components, which are seen in the contact-binary sample as a small admixture at the level of 2 percent, in their majority are not poor-thermal-contact systems but rather semi-detached binaries with matter flowing from the hotter, more massive component and forming an accretion hot spot on the cooler companion. The third paper (Rucinski 1998a = R98a) dealt with contact systems with orbital periods longer than one day. The W UMa-type sequence was shown to continue up to the orbital periods of 1.3 – 1.5 day, and then sharply terminate in this period range. The results of the three previous papers, R97a, R97b, R98a, were re-discussed in a more general comparison of the contact binaries of the Galactic Disk in the BW sample with those in old open clusters (Rucinski 1998b = R98b). It was found that the luminosity function for the contact binaries is very similar in shape to that for the solar neighborhood main-sequence (MS) stars, implying a flat apparent frequency-of-occurrence distribution. In the accessible interval $2.5 < M_V < 7.5$, the apparent frequency of contact binaries relative to MS stars was found to be equal about $1/130 - 1/100$. The resulting spatial (inclination-corrected) frequency of some $1/80$ (with a combined uncertainty of about ± 50 percent) implies a well-defined and high peak in the orbital period distribution, well above the period distribution for MS binaries by Duquennoy & Mayor (1991), extrapolated to periods shorter than one day. This peak most probably results from piling-up of short-period binaries as they lose angular momentum and form relatively long-lived contact systems.

This paper is an attempt to extend the analysis of the eclipsing systems discovered by OGLE into the pre-contact domain. In utilizing the observed period distributions, it is logically related to the studies on the orbital period evolution of tidally-locked late-type main-sequence binaries by angular momentum loss (AML) that were published in a series of papers by Maceroni and Van't Veer (1989, 1991 =MV91 ; see also see Maceroni (1999) for an update and further references). In particular, a functional form of the AML rate was derived in MV91 and Maceroni (1992) by fitting the observed period distribution of field binaries. The results nicely confirmed the need of a braking mechanism which is weakly rotation-dependent (or, perhaps, totally independent of the rotation rate) for fast rotators, but the conclusions from these analyses suffered from the unavoidable inhomogeneity of the all-sky sample. A subsequent study by Stępień (1995) arrived

at basically the same results through a very different route, via specific assumptions on the efficiency of the magnetic-field generation and an analysis of the homogeneous (but very small) sample of the Hyades binaries. Attempts to relate these theoretical predictions to the statistics of short-period binaries have so far been encountering severe limitations related to the smallness of the samples. We note that early indications that the orbital period evolution at very short periods is slower than initially expected, based on bright field-star binary statistics, were presented by Rucinski (1983), but suffered as well from low-number statistical uncertainty. The currently on-going microlensing surveys offer, for the first time, rich and homogeneous samples of binaries to overcome those limitations.

This paper uses the sample of eclipsing binaries observed by the OGLE project in the direction of Baade’s Window sample. The sample is of moderate size (933 systems) by the rapidly-evolving standards of the microlensing projects, yet it remains the only widely-available sample of that type. As we explain in Section 3, the discussion is limited – by necessity – to eclipsing binaries with almost equally-massive components. This again limits the size of the available sample. Although the results are tentative, we decided to present them for completeness and as a guidance for the future, larger surveys.

Section 2 very briefly summarizes the expected trends for the pre-contact domain while Section 3 contains the definition of the sample and its properties. Section 4 presents analysis of the observed period distribution. The last Section 5 summarizes the main results of the paper.

2. ANGULAR-MOMENTUM-LOSS EVOLUTION OF CLOSE BINARY SYSTEMS

The evolution of a close binary system crucially depends on its orbital period. When the period is short enough for an effective tidal synchronization, the angular momentum lost by the individual components through the action of magnetized wind is extracted from the orbit. The orbital separation shrinks, the components rotate progressively faster, possibly draining even more angular momentum from the orbit. Eventually, a contact system forms as a penultimate stage before merging of components and formation of a single star. This general description has been first suggested by Van’t Veer (1979), later developed by Vilhu (1982), and then explored in more detail by Maceroni and Van’t Veer (1991) and by Stępień (1995).

The implications of the angular momentum loss (AML) evolution are most obviously noticeable in the orbital period distribution. The crucial quantities here are the moment of inertia of the layers effectively braked during this process and the *rate* of the AML. The dependence of the AML rate on the rotation period, P_{rot} , or on the stellar angular velocity of rotation, $\omega = 2\pi/P_{rot}$, is frequently called the braking “law”, and is written as variants of $\dot{\omega} = \dot{\omega}(\omega)$ or $\dot{P}_{rot} = \dot{P}_{rot}(P_{rot})$. Frequently, rigid body rotation of the whole star is assumed as this simplifies derivation of the moment of inertia of the star. The detailed models of MV91 show that the tidal synchronization

mechanisms operate on such a short time scale compared to the AML one, that the hypothesis of perfect synchronization is fully justified after a few million years of evolution, so that one can write $P_{rot} = P_{orb} \equiv P$, dropping the suffixes.

The braking law is usually expressed in a parametric form of the type: $\dot{\omega} = const \cdot \omega^\alpha$, with $\alpha = 3$ for the well known Skumanich relation (Skumanich 1972) which is known to be valid for slowly-rotating, single, solar-type stars. In a perfect synchronization regime the angular momentum loss by magnetic braking $\dot{H} \propto P^{-\alpha}$ is equal to the decrease of the orbital angular momentum $\dot{H}_{orb} \propto P^{-2/3} \dot{P}$, so that the rate of change of the orbital period is $\dot{P} \propto P^{2/3-\alpha}$. The period distribution is then expected to be dependent on time, with the population of the period-distribution bins directly related to the shape of the initial distribution and to the time scale of period change.

The initial period distribution is poorly known in the short-period range of interest here. Current assumptions are extrapolations towards short periods either of the $\log P$ flat distribution of Abt and Levy (1976) (as for instance in MV91), or of the more recent one by Duquennoy and Mayor (1991 = DM91), that is derived for a relatively unbiased sample. Sometimes a short-period cut-off has been introduced, as in Stępień (1995). The DM91 distribution has the shape, in the logarithm of the period, of a wide Gaussian with a maximum at $\log P = 4.8$ and $\sigma \log P = 2.3$ (with the period P expressed in days); it can be approximated, within the range $0 < \log P < 1$ days, by $N(\log P) \propto P^{0.35}$.

The simplest case of evolution of the period distribution is that for a sample of systems all formed at the same time t_0 . If the initial distribution is $f_0(\log P)$, the evolved one at a later time t_* (e.g. the present time of observation), $f_*(\log P)$, results from the requirement of the constancy of the total number of the systems. The implied transformations of both $f_0(\log P)$, and the bin size $d \log P(t_0)$ are related through:

$$f_*(\log P) = f_0(\log P) \left| \frac{d \log P(t_0)}{d \log P(t_*)} \right| = f_0(\log P) \frac{\tau_*}{\tau_0} \quad (1)$$

which incorporates the period evolution from the time t_0 to t_* : $P_* = P_*(P_0)$. For brevity, we use P_n to signify $P(t_n)$. The quantity $\tau = |P/\dot{P}|$ is the timescale of the period evolution. Thus, from Eq. 1 we see that the present period distribution function $f_*(\log P)$ is proportional to the ratio of the present and the initial time-scales (i.e. rapid evolution will locally deplete the distribution). Obviously, in the more realistic case of the time-independent formation process over some time interval, the present period distribution would be a result of an integration of the right side of Eq. 1 over the whole time interval.

The systems of our sample cannot be considered strictly coeval: The present population of each bin presumably consists of binaries of somewhat different age reaching the relevant bin by means of the AML occurring since their formation. On the other hand, the stars in Baade's Window in their majority probably belong to a relatively old population, possibly older than ~ 5 Gyr (Ng et al. 1996, Kiraga et al. 1997), so that products of recent formation events are

quite unlikely to be seen there. In that hypothesis, and according to all the numerical models of period evolution we mentioned before, the systems presently observed as pre-contact binaries come from a initial period range where the time-scale of period change was very long and weakly time dependent for the first few Gyr of evolution. (Such a case corresponds to the period evolution functions being nearly straight and parallel to the time axis, as shown for instance in Figures 4 and 7 of MV91.) As a consequence the result of the integration over the formation time will be proportional to $f_0\tau_*/\tau_0$, where τ_0 will be a mean over the formation time. As long as we study only the shape of the period distribution we can just use the simpler expression in Equation 1.

According to the power law expressing the rate of orbital period change, the period evolution function relating P_0 to P_* can be written as:

$$P_0 = P_* \left[1 + (\alpha + 1/3) \frac{T}{\tau_*} \right]^{1/(\alpha+1/3)}$$

with $T = t_* - t_0$ and with τ_* being the present time-scale of period evolution, The present period distribution obtained from the initial distribution $f_0(\log P) \propto P_0^\beta$ will be:

$$f_*(\log P) \propto P^\beta \left[1 + (\alpha + 1/3) \frac{T}{\tau_*} \right]^{\frac{\beta - \alpha - 1/3}{\alpha+1/3}} \quad (2)$$

Figure 1 shows two examples of the evolution of an initial distribution assumed to be as a power law $f(\log P) \propto P^\beta$ with $\beta = 0.35$ (the local fit of DM91), for two values of α , 1.49 and 3; the first value corresponds to a local power-law fit of the of Stępień (1995) braking relation ($-0.5 < \log P < 1.0$), the second is the Skumanich's value (1972). In both cases identical solar-mass components were assumed.

The initial period ranges were assumed to be different for each panel; they were adjusted to correspond to intervals of initial periods that – after 8 Gyr – could populate the distribution down to 0.3 days, the approximate value of the period for contact systems consisting of solar components. In the same way only the parts of the intermediate age distributions that finally spread up to that lower boundary are shown. As can be seen from Equation 2 the evolving distribution, in a log–log plot, gradually changes its slope from the initial β to the asymptotic value of $\alpha + 1/3$. The speed of the process depends on the value of time-scale τ (and not just on its slope with $\log P$), this in its turn depends on the stellar parameters. Again, for illustrative purposes in Figure 1, we have used values derived from the Stępień and the Skumanich predictions. Writing $\tau = kP^{\alpha+1/3}$ the multiplicative constant k turns out to be $k \simeq 5.2$ and $k \simeq 0.5$, respectively for the Stępień and the Skumanich models (τ expressed in Gyr and P in days). The much shorter value of τ for the extrapolation to short periods of the Skumanich law gives a very rapid transition of the slope to the asymptotic value, and relatively long initial periods. However even with the reduced braking efficiency at short periods of the Stępień law, the short period part of the distribution very soon loses memory of the initial period distribution. We expect therefore a relatively old population of binaries, as that of Baade's Window, to contain in the short period range of Figure 1 information on the time-scale dependence of P rather than any vestiges of the initial distribution.

If the braking law were indeed as steep as implied by the Skumanich relation of Figure 1 ($\alpha = 3$), the AML evolution would progressively accelerate with a rapid shortening of $P_{rot} = P_{orb}$ as the time scale would decrease as $\tau \propto P^{10/3}$ and there would be practically no very short-period, synchronized binaries. For the solar-type dwarfs of spectral types FGK, the region around orbital periods of about 0.3 to 2 days would become quickly “evacuated”. However, there are many indications that α is definitely smaller than the Skumanich value for fast rotators, and that the braking law may, in fact, “saturate”, converging to a constant. Then, the rate of the evolution would still depend on the period, but with a much shallower slope ($N \propto \tau \propto P^{1/3}$ for the limiting value of $\alpha = 0$) and longer τ .

The strongest dependence on the AML efficiency is in any case expected to take place at the very short end of the period distribution. Presumably some temporary increase in the number of very short-period systems that formed with longer periods may occur there, but – over time – the distribution will reflect the AML efficiency as the distribution evolves into the steady state determined by the braking time-scale. At the very short period end one expects a prominent effect of truncation as the close detached systems become converted into contact binaries. The final piling in the contact binary domain is very clearly seen in the currently most extensive statistical data for the Galactic Disk contact binaries visible in the Baade’s Window direction (R98b).

Figure 2 compares these data with the extrapolation of the DM91 period distribution to very short periods. Validity of such an extrapolation is put in question by a small but homogenous sample of dwarfs in the young cluster of Hyades (Griffin 1985) where an increase in star numbers toward short periods within the range $1 < P < 10$ days is actually observed (see Figure 2). Although the statistics for the Hyades binaries is poor, the trend is quite obvious. It is not clear if this is a remnant of the formation process or an indication that the AML evolution actually *slows down* at very short periods due to the inversion in the braking efficiency (negative α). Such a possibility is not entirely excluded as the rapid-rotation regime is very poorly understood in terms of the AML efficiency. For example, presence of thinly-populated “tails” of extremely rapidly-rotating late-type dwarfs in young clusters (Hartmann & Noyes 1987) may indicate such an inverted AML efficiency. Besides, very close-binary stars do not have to behave exactly as single stars due to the influence of the tidal effects on the magnetic field generation modes.

In summary: The value of the exponent α in the braking efficiency law, $\dot{H} \propto P^{-\alpha}$, for the high rotation-rates in close binary systems is currently a very poorly known quantity so that any observational results which are free of systematic effects, would be of great value. An estimate on α was the goal of the present paper.

3. THE SAMPLE OF PRE-CONTACT SYSTEMS

3.1. Definition of the sample

The extraction of the sample of pre-contact systems is not a trivial matter, given the limited photometric information for the periodic variable stars in the OGLE catalog. The availability of only single color light curves is particularly inconvenient because – without color curves – we could not eliminate the semi-detached Algols, which are particularly easy to detect (due to deep primary minima) and are thus expected to dominate in number over the Main Sequence stars in surveys similar to OGLE. Of course, Algols can be recognized, even from a single color light curve, thanks to their characteristic large difference of depth of the minima. One can eliminate them, as we did, by applying a criterion of equal eclipse depth, but this introduces a restrictive limitation to systems with components having similar effective temperatures. On the Main Sequence, this criterion is basically equivalent to selection of binaries with similar components, i.e. with mass-ratios ($q = M_2/M_1 \leq 1$) close to unity ($q \simeq 1$). Such systems may still be numerous; for example the shortest-period currently known Main Sequence binary, BW3.038¹, at the very short-period end of our distributions is such a system (Maceroni & Rucinski 1997 = MR97). Nevertheless, a limitation to the mass-ratios close to unity may be considered a drawback in our approach. However, it was inevitable, in view of the very limited information of single-color light curves that we had in our disposal.

The “pre-contact binary” light-curve shape filter that we used is based on the Fourier cosine series decomposition of the light curves. The basic philosophy of the approach follows the principles of the filter used to select a sample of contact binaries described in R97a and R97b (consult in particular Figure 5 in R97a). The first coefficient, a_1 , reflects the difference between the two eclipses and for equally-deep minima goes to zero; the second, a_2 is the largest of the coefficients and represents the total amplitude of the light variations; a_4 measures the eclipse “peakedness” and goes to small values for the light curves of contact systems. As was shown in R97a, the pair (a_2 , a_4) forms a powerful separator/discriminant of contact/detached binaries.

The procedure to select our sample of short period pre-contact systems required a few steps. By means of the contact/detached binaries filter of R97a, a first sample of all the non-contact systems (339 objects) was selected. These are the systems falling above the “contact line” in the a_4 *vs.* a_2 plane, in the left panel of Figure 3.

The application of the shape filter based on the a_1 coefficient, to keep only binaries with similar eclipse depths, is shown in the right panel of the same figure. This step involves the selection of systems with similar components. The equal eclipse-depth criterion implies the retention of values of a_1 close to zero. A reasonable lower limit on a_1 , and hence a maximum allowed difference of the minima can be decided by inspection of the a_1 distributions which are

¹The naming convention used here is the same as in the previous papers of this series: BW for Baade’s Window (these letters are sometimes omitted), followed by the OGLE field number, and then the variable number, after the dot. The central field BWC is identified by zero.

shown in the two left-side panels of Fig. 4. The lower panel shows the distribution of the current sample of 339 detached binaries while the upper one is for the contact binaries of the R-sample in R97a. The R-sample is composed by W UMa binaries with very similar effective temperatures and thus equally-deep minima, hence the distribution peaks at small $|a_1|$. In contrast to the R-sample of contact binaries, the distribution of a_1 for our sample of detached systems is strongly bimodal. The comparison of the two distributions suggests that similar depths of eclipses are selected for a limiting value of $a_1 \geq -0.017$. This criterion establishes, however, only a necessary condition, as a_1 is not only temperature-difference dependent but also approximately scales with the light curve amplitude. A filter based only on a_1 , would pass, therefore, many low-amplitude light curves for systems with low orbital inclination, but appreciable temperature difference. Since the second Fourier coefficient a_2 is related to the light curve amplitude, the simplest way to take the light-curve amplitude scaling into account is by means of the ratio $r = a_1/a_2$. The distribution of r for the same samples of contact and detached binaries is shown in the right panels of Figure 4. A reasoning similar to that given above for the a_1 distributions suggests a threshold value of $r_{max} = 0.2$. The selection on the depth difference has been done, therefore, using both conditions.

A special comment is needed for the few systems with positive values of a_1 , and hence negative values of r (a_2 is always negative). By definition (see R97a), a_1 is negative for a light curve where the primary minimum is the deepest one. The OGLE team assigned the primary eclipses to the deeper minima, as is customary for eclipsing variables, so that a_1 should in principle be always negative. Positive a_1 's can, therefore, be only due to errors introduced either in this assignment or in the calculation of the Fourier coefficients; the latter circumstance may result from large photometric errors or because of a poor or uneven light-curve phase coverage. The presence in Figure 4 of several points at $a_1 > 0$, requires a criterion for rejection of the positive a_1 's as well. Otherwise the poor light curves would be favored with respect to the good-quality ones. We decided, after a check of the light curves of the most extreme cases, that the pure rejection of positive a_1 systems would not be justified, as some curves were indeed of rather poor quality, but of the expected shape. The simplest choice was therefore to apply the previously defined limits on a_1 in its absolute value. The selection was then performed according to: $|a_1| < 0.017$ and $|r| < 0.2$. This additional constraint does not change the sample in a significant way as only four systems are rejected, but improves the consistency of the selection.

One of the four systems rejected at this stage, BW5.173, is a potentially interesting object for further studies. It is a faint binary ($I = 17.82$) with an orbital period $P \simeq 0.66^d$ and the light curve of a well-detached system with components of similar effective temperatures. After the de-reddening procedure (see Section 3.2), it turns out, with $(V - I)_0 = 2.28$, to be the reddest system of the whole sample of detached binaries, with an absolute magnitude $M_I = 7.55$ and a distance $d = 791$ pc. Thus, the system seems to be very similar to BW3.038, i.e. it consists of a pair of M-type dwarfs, but with a period three times longer. Since such eclipsing systems are rare, the system is of significance as it increases the small number of the potential calibrators of the red end of the main sequence.

In addition to the light-curve shape filter described above, a physical condition on the orbital period was used as the final step in the sample-definition to eliminate the rare systems with evolved components. These can be easily recognized by their relatively long periods, so we set an upper limit of $P = 8^d$ as a reasonable value for tidally locked binaries with MS components. The systems selected through all the criteria described above are marked by filled symbols in Figure 3, which shows the details of our Fourier filter.

The sample of systems selected through the light-curve filter and the period criterion $P < 8^d$ has been further checked for presence of systems which could deteriorate the quality of the sample. In particular, the Fourier coefficients for systems with partially-covered light curves may be entirely erroneous. Visual examination of the light curves led to removal of two systems BW2.072 and BW4.099. After removal of six further systems without measured $(V - I)$ colors, the sample consisted of 77 systems. All these, except three rejected because of too blue intrinsic colors (see Section 3.2), formed the final sample of 74 systems used in this paper. The systems are listed in Table 1, where – in addition to the original OGLE data of the period, P , the maximum magnitude and color I and $(V - I)$, and the amplitude ΔI – we give the derived values (see below): the absolute magnitude M_I , the de-reddened color $(V - I)_0$ and the distance in parsecs, d . The Fourier coefficients are available from the authors through their respective Web pages².

3.2. Properties of the systems in the sample

Additional information on the properties of the systems came from the consideration of their absolute magnitudes and de-reddened colors. These were derived by an iterative process of distance determination, in an approach somewhat similar to that described in R97a, and identical to that used in the study of the system BW3.038 (MR97).

The procedure was as follows: An adopted absolute-magnitude calibration $M_I = M_I((V - I) - E_{V-I}(d))$ for the main sequence was used to find the distance d and reddening E_{V-I} . The procedure was iterative with the reddening allowed to vary linearly with distance between zero and the maximum value derived from the background Bulge giants by Stanek (1996), assuming that E_{V-I}^{max} is reached at the distance of 2 kpc, and then does not increase. The adopted MS relation was that of Reid and Majewski (1993), but with a shift by 0.75 magnitude to allow for two identical stars, in consistency with the definition of the sample of $q \simeq 1$ systems. The results of the approach are the de-reddened colors, $(V - I)_0$, the distances d and the absolute magnitudes, M_I (see Table 1).

The intrinsic colors of three system, 7.004 with $(V - I)_0 = 0.21$, and 1.221 and 6.081, both with $(V - I)_0 = 0.44$ were found to be too early for consideration in the sample of late-type stars.

²The tables of Fourier coefficients for all 933 binaries discovered by the OGLE project are located in <http://www.astro.utoronto.ca/~rucinski/ogle.html> and <http://www.mporzio.astro.it/~maceroni/ogle.html>

The elimination of those three systems led to the reduction of the sample to 74 systems. The intrinsic color distribution (Figure 5) shows most of the systems in the range $0.6 < (V - I)_0 < 1.3$ with a tail extending to red colors. One may expect that M-type dwarfs populating the tail may have different AML properties than the FGK-type stars. Thus, we separately considered 64 systems with $(V - I)_0 < 1.3$ and 10 systems with redder colors. The border line is located approximately at the spectral type K5V.

The division into the two spectral groups was dictated not only by the possibility of the different regime in the AML, but also because the sampled spatial volumes are expected to be vastly different as a function of absolute magnitudes, leading to a possibility of very different discovery selection effects. We can gain some insight into the matter of the spatial depth of the samples by consideration of the increase in the number of stars with the distance. Figure 6 shows the logarithmic plots of the cumulative number of stars versus the distance for both groups. For the Euclidean geometry, the slope is expected to be 3, which is approximately fulfilled by the nearby M-dwarfs. For the FGK-type stars we see a definite deficit at small distances, then the expected increase in number and then a strong cut-off at about 3 kpc. The deficit at small distances is due to the bright limit of the OGLE sample at $I = 14$, while the cut-off at large distances is due to the combination of the faint limit of the OGLE sample and of the line-of-sight leaving the galactic disk (see Section 9.1 in R98b). The cut-off is relatively sharp because 72 and 92 percent of stars of the FGK group are located closer than 3 kpc and 4 kpc, respectively.

The main goal of this paper is the derivation of a statistically sound orbital-period distribution. This distribution may – and probably does – depend on the spectral type range, but with the small number of systems we cannot avoid the necessity of grouping the systems into relatively coarse samples. We therefore check first if the division into only two broad spectral groups is a legitimate one and whether the range of colors in the FGK group is not selected too wide.

Previous studies on all-sky samples in the same period range suggested a change in the period distribution which is dependent on the spectral type, although the division seems to be located between early A–F and late G–M type binaries. The distributions of about 1200 close binaries in the sky field, grouped by spectral type of Farinella et al. (1979) show a change in shape from unimodal, for systems with O–F type components, to bimodal for G types, and to multimodal for K–M spectral types. A later study by Giuricin et al. (1984), of 600 eclipsing and spectroscopic field binaries also shows – though less clearly defined – a trend towards broader distributions for later spectral types. These large field samples are, however, so heterogeneous that is practically impossible to deal with the many selection effects and misclassifications affecting them. The current small, but homogeneous one, provides a totally independent and external check on these results.

A first test of the homogeneity of our sample of 74 systems was done by splitting it into color-range defined subsamples. In this test, we tried two partitions: into two equal-size samples of 37 systems each (containing systems respectively bluer and redder than $(V - I)_0 = 0.93$), and

into two sub-samples of FGK and M binaries, as defined above (the division at $(V - I)_0 = 1.3$). The null hypothesis of the same parent population was checked by means of a standard two-sided Kolmogorov-Smirnov test, by computing the maximum absolute difference between the two cumulative distributions, D_{KS} , and the significance level of the null hypothesis P_{KS} . The cumulative period distributions are shown in Figure 7. We see some subtle differences between the sub-samples, but – taking into account the small number of objects in the sub-samples – they are not significant to the point of rejection of the null hypothesis of the same period distribution. We note that for the equal-number division, the blue sub-sample extends from 2 to 6 kpc while the red one extends only from 0.5 to 3 kpc so that different discovery selection biases are not excluded. The results of the KS test, reported in Table 2, do not allow firm conclusions: The significance levels for both divisions are close to 0.6; the differences are probably mostly due to systematic trends in discovery selection effects, but – at least – the results indicate that the null hypothesis cannot be rejected.

Similarly to the cumulative period distributions, no obvious dependences are visible in the scatter diagrams for the $(V - I)_0$ vs. $\log P$ and M_I vs. $\log P$ relations, as shown in Figure 8. This is confirmed by the values of the correlation coefficients which are all close to zero. The results of application of the Kendall (r_K) and Spearman rank (r_S) correlation coefficients are given in Table 2. We should note that although M_I is partly derived from $(V - I)_0$, it also depends on I so that the correlation coefficients given in the table do not have to be exactly same, as they appear to be.

The lack of correlation between periods and colors or absolute magnitudes is the reason why no attempt at the definition of a volume-limited sample (say to 3 kpc) was made, thus allowing inclusion of more distant systems as well. We retained partition into the FGK and M groups, however, entirely on the basis of an expectation that the M-dwarf sub-sample may have different AML properties. For that reason, we consider in this paper both, the FGK group of 64 systems as well as the full sample of 74 systems. Obviously, the M-dwarf group is too small for any separate period-distribution considerations.

4. THE PERIOD DISTRIBUTION AND DISCOVERY SELECTION BIASES

4.1. The orbital-period distribution

We have used the sample of 64 FGK-type binaries and then the full sample augmented by 10 M-type binaries to analyze the orbital period distribution and thus infer the AML-driven orbital-period evolution in the pre-contact stages. The implicit assumption was that the orbital periods and mass-ratios are not correlated. In the opposite case, the pre-selection of $q \simeq 1$ systems might lead to a bias in the period distribution.

The observed period distributions, for the whole sample of 74 systems and for the FGK

group of 64 systems, are shown in Figure 9. Except for very short periods, $P < 0.35$ day, where no detached FGK binaries could exist because of the onset of contact, the data show a trend of progressively decreasing number of binary systems for increasing period. Weighted fits to the histograms of $\log N$ versus $\log P$ (Figure 9 in the form: $\log N = A_0 + A_1 \log P$, with weights calculated on the basis of Poissonian errors in bins $\Delta \log P = 0.2$ wide, gave $A_0 = 1.05 \pm 0.06$, $A_1 = -0.79 \pm 0.16$ for the whole sample, and $A_0 = 1.02 \pm 0.07$, $A_1 = -0.80 \pm 0.17$ for the FGK sub-group. The values of χ^2 for the fits were 3.1 and 3.7 for the 6 log-period bins. The linear fits are thus only marginally appropriate, but definitely much better than flat distributions.

To define the uncertainty limits on the coefficients A_0 and A_1 , a Monte-Carlo experiment has been conducted in which weighted fits were made to several thousand artificial Poisson distributions with the same *mean* values for each log-period bin. Because the mean values do not form a linear dependence, such fits provide more realistic estimates of the uncertainties of the coefficients A_0 and A_1 . The results, expressed in terms of the distributions of the individual determinations of the coefficients around their median values, are given in Table 3. The fits are shown in the second panel of Figure 9.

The linear fits in Figure 9 show an unexpected slope as the number of systems decreases, rather than increases with period. Even for a “saturated” AML rate (see Section 2) the slope should be the opposite of what is found. For any $\alpha \geq 0$ in $\dot{H} \propto P^{-\alpha}$ the logarithmic slope of the number distribution should be larger than $1/3$, as in $N \propto P^{\alpha+1/3}$. In other words, the short-period end of the period distribution for pre-contact binaries should be always less populated.

We think that the observed trend, which is contrary to the expectations, is entirely due to discovery-selection bias effects scaling in proportion to the period length. For the first time we have a well-defined sample of eclipsing systems and for the first time we can see the selection effects so clearly, without other discovery biases. There are several reasons why systems with longer periods are more difficult to detect: (1) Chances of observing eclipses decrease with the increasing separation of the components, as the range of orbital inclinations rapidly shrinks; (2) Chances of detecting eclipses decrease as they become progressively shorter; (3) Fewer orbital cycles and thus fewer eclipses are observed for a given duration of the survey.

The only rigorous approach in handling the detection biases would be to simulate the whole discovery process, starting from the data-taking through all the following reduction stages. Such simulations could be done only by the OGLE team. Since they are not available, simplified approaches of handling the discovery selection have been attempted.

4.2. Orbital-period selection biases

The discovery selection biases can be estimated by consideration of probability that a distant observer notices eclipses. One way to estimate this probability is by evaluating the solid angle subtended by the sum of the fractional radii $(r_1 + r_2)/a$, relative to hemisphere visible by a distant

observer, i.e. by dividing it by 2π steradian. This relative solid angle is given by the integral of the eclipse relative durations over the range of inclinations that can result in eclipses, which evaluates to $1 - \left(\sqrt{1 - \left(\frac{r_1+r_2}{a} \right)^2} \right) \approx \left(\frac{r_1+r_2}{a} \right)^2$. For fixed radii, the probability of discovery of an eclipsing system scales as the inverse of its orbital separation in square, $\propto a^{-2}$. The same proportionality is obtained by considering the fraction of the sky one star “sees” covered by the other star. Obviously, such very simple estimates only very approximately represent trends in the depth and duration of the eclipses, as seen by a distant observer, but do show that the discovery selection effects rather strongly depend on parameters of binary systems.

Below, we will take a pragmatic approach and consider other “strengths” (other power-law dependences) of the discovery biases, but we feel that the discovery-probability scaling according to a^{-2} should be a particularly reasonable assumption for the equal-mass, hence presumably equal-radius component systems that we selected. The correction factor that we should use to multiply the statistics of periods is then expected to behave as: $corr \propto a^2 \propto M_{tot}^{2/3} P^{4/3}$. The mass dependence can be further removed by observing that, as we described in Section 3, the orbital periods in our sample do not correlate with the color or absolute magnitude. We can therefore assume that they do not correlate with the total mass of the system, M_{tot} . The correction factor to apply to the histograms in Figure 9 would be then: $corr \propto P^{4/3}$. Since we considered the logarithmic slopes in fitting the $\log N$ versus $\log P$ dependences, we will from now on – instead of $corr$ – use the slope correction C , as in $corr \propto P^C$, with the most likely value of $C = 4/3$.

The relation between the braking-efficiency exponent, α , the observed slope, A_1 , and the observational selection correction, C is: $\alpha = A_1 + C - 1/3$. We will consider implications of assuming various values of C . For the value of A_1 , we have a choice of selecting between the directly determined values of $A_1 = -0.79$ or -0.80 , or from the Monte Carlo experiment, $A_1 = -0.74$ or -0.73 . For simplicity, and because any results will in fact be dominated by the systematic effects characterized by C , we set – from now on – $A_1 = -0.75 \pm 0.20$ (the error estimate comes from the Monte Carlo experiment, see Table 3). Some illustrative cases are discussed below:

C = 0: This is a case of no discovery selection effects. This case is hardly possible, not only because the detection biases almost certainly exist, but also because we obtain then a strongly inverted braking efficiency law with $\alpha = -1.08$. This would imply that rapidly rotating stars lose relatively less angular momentum than the slowly rotating ones.

$\alpha = 0$: A perfectly “saturated” law dH/dt with no dependence on the period. The bias correction would be then $C = +1.08$ which is only slightly less than the most preferred by us value of $4/3$. We also that evolution would in this case produce almost no change of the initial slope (going from a value of $\beta = 0.35$ to $\alpha + 1/3 = 1/3$).

C = +4/3: This is our preferred value of the bias resulting in the value of $\alpha = +0.25$, i.e. close to saturation, yet with a weak acceleration of the AML evolution with shortening of the period.

C > +1.75: This inequality is considered here following the theoretical arguments of Stępień

(1995) that $\alpha - 2/3 > 0$ (see his Figure 1), (a particular value in this range is the local fit of the braking law, as used in Figure 1 that yields $C = 2.57$). These solutions would imply that the current sample suffers from stronger discovery selection biases than expected for $C = 4/3$.

In conclusion, we feel that the most likely value of the AML braking-law exponent is close to $\alpha \simeq 0$. The discovery selection effects are strong and important, yet the departure from the bias exponent $C \simeq 4/3$ would imply implausible combinations of parameters. For $C = 0$, the period distribution would have a genuinely negative slope, with more binaries accumulating at the short-period end of the period distribution, just before the conversion into contact binaries. We note that such a law would agree with the statistics of short-period systems in Hyades (Griffin 1985; see Figure 2 in Section 2), provided, of course, that it does not have its own detection biases. However, it is really hard to imagine that the discovery biases do not exist in the OGLE database, so that almost certainly $C \geq 0$. Applying progressively larger corrections C would make α closer to zero and then positive. If $C > 4/3$, then the discovery biases would be exceptionally strong. We cannot exclude this possibility, but consider it unlikely.

The referee of the first version of the paper pointed out that a saturated braking law extending to periods as long as our upper limit may be in disagreement with the results for late-type single stars. The activity indicators that can be related to the AML rate show a change of slope – from a saturated to a steeper law – at rotation periods around 3–4 days (see for instance Wichmann et al. 1998). A mass-dependent slope transition (from $P \approx 2^d$ for $m = m_{\odot}$ to $P \approx 9^d$ for $m = 0.5m_{\odot}$) was included in the theoretical models of Bouvier et al. (1997) and found to provide a good fit of PMS and MS rotational data. The small size of our sample and the consequent relatively coarse binning did not allow us to properly analyze this feature. The expected change of the slope would fall in the tail of our distribution since we currently have only three systems in the bin $P > 5$ days. On a qualitative ground, Figure 9 does suggest that an exclusion of the last bin from the fit would result in a slightly flatter braking law, but we feel that an estimate of the slope based on such reduced data would actually be an over-interpretation of the available material.

5. DISCUSSION AND CONCLUSIONS

We have used the by-product of the OGLE microlensing project, the database of eclipsing binaries toward Baade’s Window, to analyze the period distribution of short-period ($0.19 < P < 8$ days), late-type, main-sequence systems. This distribution was used to shed light on the angular-momentum-loss efficiency for rapidly-rotating, late-type stars. The final results are very tentative as they are totally dominated by the systematic effects of discovery biases. Yet, they may be of importance for similar future applications of microlensing databases, so that certain lessons can be learned from our experiences.

The main, obvious lesson is thus a very high importance of testing the variability-discovery

algorithms for period-length biases. This can be done only by the observing teams, by simulations of detectability of variable stars. Any a posteriori corrections to the observed statistics have debatable value, as is the case with our slope correction C , introduced in Section 4. Depending on its value, we can obtain any braking law $dH/dt \propto P^{-\alpha}$, with $\alpha = -1.1 + C$. We tend to favor a relatively strong detection bias law described by $C = +4/3$ and (implying a braking law close to the “saturated” one of $\alpha \simeq 0$), but any value of C is basically permissible. It seems very unlikely that $C = 0$, that is that the OGLE database has no period biases. For this case, however, the negative slope of the braking law would agree with the statistics of short-period binaries in Hyades (Griffin 1985), with more binaries at the short-period end.

The other lesson is the availability of color curves. Because the light curves were observed in one color only, we had to use a very strong light-curve-shape criterion to filter out the easily-detectable Algols and define a sample of short-period, main-sequence systems with almost identical components. The sample that we defined consists of 74 objects, but would be larger if all systems with MS components having un-equal temperatures were not rejected. Because of this restriction, we could not meaningfully consider any quantities related to spatial frequency of occurrence (such as luminosity or period functions discussed extensively for the OGLE contact systems in R98b). This resulted in a limitation that the available quantity was the slope of the period distribution, and even that affected by strong discovery selection biases.

We note that our sample of 74 systems consisted of 64 binaries of spectral types F, G and K and 10 M-type systems with a large spread in colors. We expected differences in properties between these samples and thus considered them separately, but did not notice any major disparities which would affect the period-distribution statistics.

In addition to these somewhat general statements, we add a minor, but firmer conclusion that there exists no evidence in our homogeneous sample for any bimodal period distribution, similar to that found by Farinella et al. (1979) with a dip at $\log P \simeq 0.2$. We feel that this dip and a secondary maximum in the distribution were most probably produced by misclassification of evolved systems as consisting of main-sequence components. A smooth period distribution, without any structure, implies a different form of the braking law with respect to that derived by MV91 and Maceroni (1992). Though the functional form remains similar, in the sense of a “saturated” braking at short orbital periods ($\alpha = 0$), the other main feature, namely the sudden increase of the braking efficiency for rotation of $\sim 10\omega_{\odot}$ is no longer mandated by the data. That feature was needed to reproduce the bimodal distribution of field G-type systems, that had a pronounced dip around $\log P = 0.2$ days in the distribution of Farinella et al. (1979).

We would like to acknowledge the OGLE team for the access to their database.

This work was partially supported by research grants to CM of the Italian MURST (Ministry of University, Scientific and Technological Research) and of the Italian Space Agency. This work was started by SMR during his employment by the Canada-France-Hawaii Telescope.

REFERENCES

Abt, H. A., & Levy, S. G. 1976, *ApJS*, 30, 273

Bouvier, J., Forestini, M., & Allain, S., 1997, *A&A*330, 521

Duquennoy, A., & Mayor, M. 1991, *A&A*, 248, 485 (DM91)

Farinella, P., Luzny, F., Mantegazza, L., & Paolicchi, P. 1979, *ApJ*, 234, 973

Giuricin, G., Mardirossian, F., & Mezzetti, M. 1984, *ApJS*, 54, 421

Griffin, R.G. 1985, in *Interacting Binaries*, eds. P.P. Eggleton and J.E. Pringle, Reidel, Dordrecht, p.1

Hartmann, L.W., & Noyes, R.W. 1987, *ARAA*, 25, 271

Kiraga, M., Paczynski, B., & Stanek, K.Z. 1997, *ApJ*, 485, 611

Maceroni, C. 1992 in *Inside the Stars*, W. Weiss & A. Baglin Eds, *ASP Conf. Ser.* 40, 374.

Maceroni, C. 1999, *New Astronomy*, in press

Maceroni, C., & Rucinski, S.M. 1997, *PASP*, 109, 782 (MR97)

Maceroni, C., & Van 't Veer, F. 1991a, *A&A*, 246, 91 (MV91)

Morbey, G.L., & Griffin, R.F. 1987, *AJ* 417, 343

Ng, Y.K., Bertelli, G., Chiosi, C., & Bressan, A. *A&A*, 310, 771

Reid, N., & Majewski, S. R. 1993, *ApJ*409, 635

Rucinski, S.M. 1983, *Observatory*, 103, 280

Rucinski, S.M. 1997a, *AJ*, 113, 407 (R97a)

Rucinski, S.M. 1997b, *AJ*, 113, 1112 (R97b)

Rucinski, S.M. 1998a, *AJ*, 115, 1135 (R98a)

Rucinski, S.M. 1998b, *AJ*, 116, 2998 (R98b)

Skumanich, A., *ApJ*, 171, 565

Stanek, K. Z. 1996, *ApJ*, 460, L37

Stępień, K. 1995, *MNRAS*, 274, 1019

Udalski, A., Kubiak, M., Szymanski, M., Kaluzny, J., Mateo, M., & Krzeminski, W. 1994, *AcA*, 44, 317

Udalski, A., Szymanski, M., Kaluzny, J., Kubiak, M., Mateo, M., & Krzeminski, W. 1995a, *AcA*, 45, 1

Udalski, A., Olech, A., Szymanski, M., Kaluzny, J., Kubiak, M., Mateo, M., & Krzeminski, W. 1995b, *AcA*, 45, 433

Van 't Veer, F. 1979, *A&A*, 80, 287

Van 't Veer, F., & Maceroni, C., 1989, A&A, 220, 128
Vilhu, O. 1982, A&A, 109, 17
Wichmann, R., Bouvier, J., Allain, S., & Krautter J., 1998, A&A330, 521

Captions to figures:

Fig. 1.— The figure shows the expected evolution of the period distribution for two values of α , 1.49 and 3, following the theoretical predictions of Stępień (1995) and Skumanich (1972). The starting distribution in both cases have the same, gently-positive slope $\beta = 0.35$, as in $f_0 \propto P^\beta$. The initial period ranges are different for each panel; they have been adjusted to populate the distribution down to 0.3 days after the time interval of 8 Gyrs. The numbers by the lines give the ages of the respective populations in Gyr. The short vectors in the left parts of the panels give the asymptotic slopes $\alpha + 1/3$, as expected from considerations in the text.

Fig. 2.— The observed period distribution for contact binaries of the disk population (the solid-line histogram and left vertical axis), based on the R98b results and the data for Hyades dwarfs (Griffin 1985; the broken-line histogram and right vertical axis) are compared here with the shape of the extrapolated DM91 distribution of DM91 (thin-line curve). Note that the statistics for the contact binaries is based on about one hundred objects (the long-period side of the peak is actually based on more than 200 objects), whereas the number of short-period binaries observed in Hyades is a dozen or so, so that the statistics is quite uncertain.

Fig. 3.— The Fourier-coefficients a_1 , a_2 and a_4 formed the main part of the shape filter utilized to select short-period pre-contact systems, as described in the text. The systems accepted for the final sample are marked by filled symbols.

Fig. 4.— The distributions of a_1 (left panels) and a_1/a_2 (right panels) for two samples: for 339 detached binaries (lower panels), and for the R-sample of W UMa contact binaries as selected in R97a (upper panels) are shown here to illustrate different properties of the contact and detached binary samples. The dotted lines show the limits that have been chosen by comparison between the distributions of the two samples to select binaries with equal-temperature (and, presumably, equal-mass) components.

Fig. 5.— The color distribution for the whole sample of pre-contact systems. The border between the two spectral groups was fixed at $(V - I)_0 = 1.3$.

Fig. 6.— The cumulative number distributions with distance of systems for the FGK and M groups are shown by full-line and broken-line histograms. The thin lines give the uniform density relations with the Euclidean slope of 3.

Fig. 7.— Left panel: the cumulative relative distribution with period of two equal size samples of 37 systems grouped by color, systems bluer (full line) and redder (broken line) than $V - I = 0.93$. Right panel: the cumulative relative distribution of 64 FGK and 10 M-type systems (full and broken line).

Fig. 8.— The scatter diagrams illustrating lack of correlation between the orbital period and the color (left panel) or the absolute magnitude (right panel). The two spectral groups are marked by

filled (FGK sample) and open (M sample) symbols. Note that the absolute magnitudes are for the combined brightness of the components which were assumed to be identical.

Fig. 9.— The orbital period statistics in linear (left panel) and logarithmic (right panel) units of the number of systems in bins $\Delta \log P = 0.2$. The histograms are shown for the full sample of 74 systems (solid lines) and the FGK group of 64 systems (dotted line), but – for clarity – the Poisson errors are shown as vertical bars for the full sample data only. The sloping lines in the logarithmic (right hand side) panel show the linear fits, as described in the text.

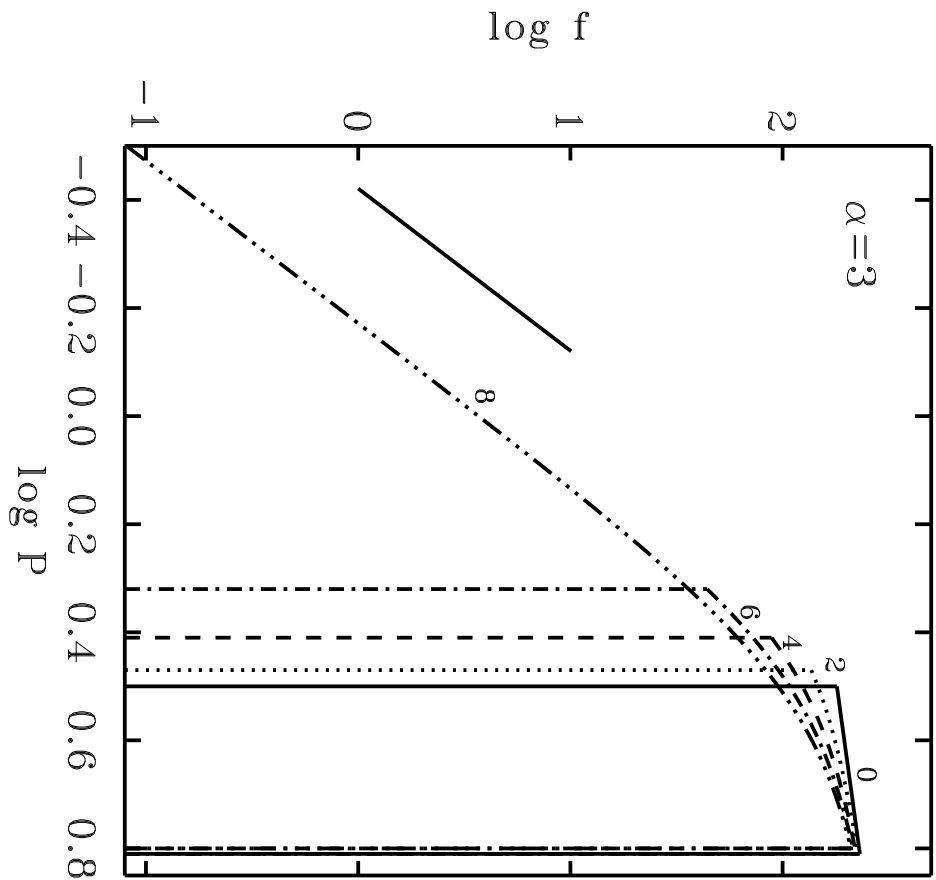
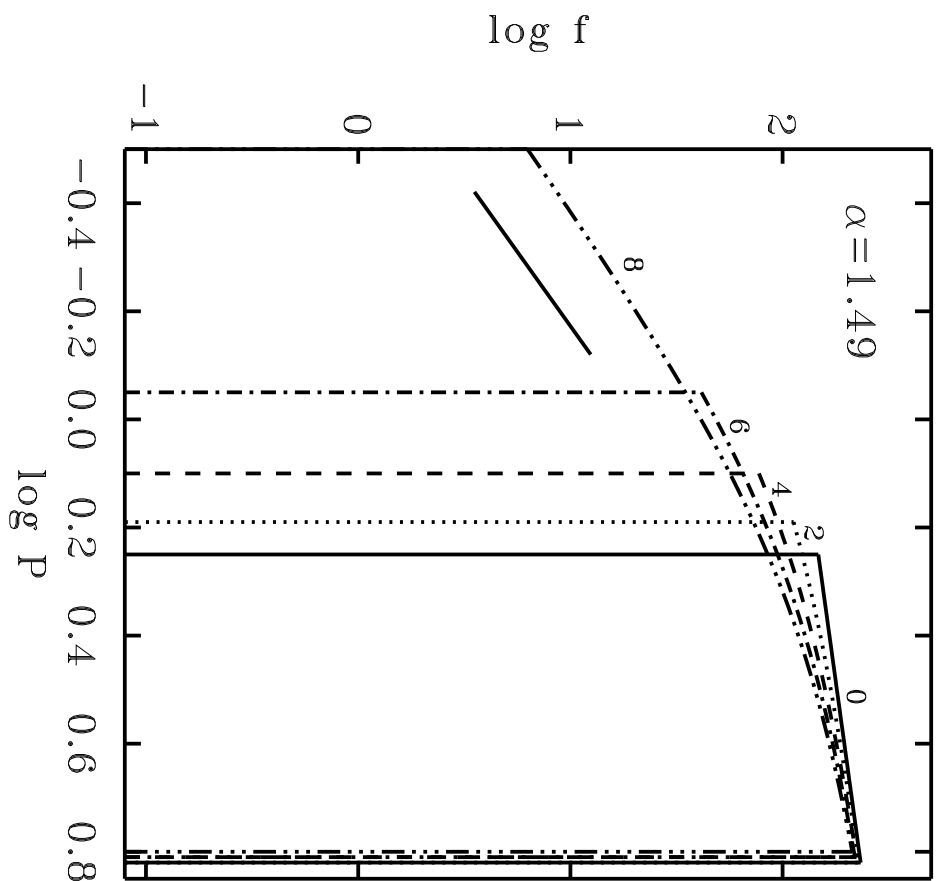


TABLE 1. Pre-contact, equal-mass systems in the OGLE sample

Name	$P(\text{d})$	I	$V - I$	ΔI	M_I	$(V - I)_0$	d(pc)
0.064	6.14613	15.82	1.93	0.31	6.14	1.69	730
0.080	0.70392	16.18	1.87	0.12	5.88	1.58	938
0.098	0.45720	16.44	1.36	0.13	3.21	0.66	2690
0.156	1.84553	17.21	1.37	0.53	3.82	0.80	3208
0.168	0.58226	17.32	1.65	0.20	4.57	1.02	2312
0.187	0.50304	17.52	1.75	0.53	4.80	1.12	2280
0.197	0.37862	17.64	1.44	0.35	3.99	0.84	3568
1.073	1.35409	16.25	1.24	0.31	2.95	0.60	2945
1.136	0.66193	17.01	1.15	0.32	2.66	0.53	4859
1.145	0.37796	17.06	1.21	0.15	2.93	0.60	4326
1.166	0.24876	17.28	1.62	0.21	4.50	1.00	2340
1.197	2.72157	17.56	1.84	0.21	5.01	1.21	2098
1.202	3.79120	17.59	1.82	0.32	4.96	1.19	2158
1.208	0.84535	17.66	1.56	0.31	4.48	0.99	2893
1.213	1.28863	17.73	1.52	0.33	4.18	0.88	3319
2.092	0.58462	16.94	1.34	0.33	3.30	0.68	3351
2.102	2.37864	17.04	1.62	0.30	5.98	1.62	1630
2.128	0.65208	17.28	1.89	0.35	4.58	1.03	1889
2.149	0.41874	17.56	1.62	0.22	4.39	0.95	2698
2.159	1.10732	17.68	1.95	0.70	5.16	1.28	2003
3.038	0.19839	15.83	2.45	0.78	7.51	2.26	406
3.132	0.81843	17.09	1.51	0.36	3.85	0.81	2667
3.158	0.41977	17.44	1.76	0.20	4.58	1.03	2233
3.162	0.53450	17.49	1.45	0.75	3.84	0.81	3384
3.163	3.04952	17.49	1.50	0.50	3.95	0.83	3181
3.175	0.41234	17.59	1.86	0.46	4.00	0.84	2531
3.196	0.35700	17.78	1.50	0.52	3.56	0.74	4053
4.030	0.25826	15.68	1.20	0.10	2.65	0.53	2585
4.073	5.43115	16.37	1.66	0.79	4.99	1.20	1389
4.160	0.39955	17.40	1.61	0.24	4.35	0.93	2575
4.170	0.38105	17.50	1.44	0.21	3.79	0.79	3563
4.176	0.38976	17.53	1.68	0.21	4.33	0.92	2661
4.204	2.54712	17.77	1.76	0.47	4.74	1.10	2590
5.081	0.48757	16.46	2.14	0.14	6.56	1.86	791
5.085	2.05045	16.54	1.36	0.26	3.20	0.66	2857
5.096	1.43270	16.85	1.35	0.40	3.11	0.64	3419
5.111	0.44486	17.02	1.95	0.19	5.64	1.48	1363
5.149	1.31085	17.57	2.11	0.93	5.95	1.61	1486
5.150	0.39329	17.60	1.58	0.31	4.41	0.96	2823
5.158	0.33036	17.67	1.69	0.31	4.42	0.96	2669
5.165	0.42679	17.77	1.88	0.46	4.40	0.95	2488
5.171	2.31344	17.83	1.97	0.41	5.11	1.25	2114
6.097	1.47660	17.07	1.49	0.27	4.04	0.85	2553
6.099	5.50434	17.08	1.50	0.36	3.83	0.80	2732
6.112	2.65984	17.27	1.69	0.49	4.53	1.01	2167
6.115	0.40963	17.29	1.65	0.21	4.34	0.93	2365
6.124	0.39862	17.39	1.65	0.19	4.42	0.96	2432
6.134	0.38820	17.56	2.09	0.24	5.87	1.57	1514
6.136	0.44347	17.64	1.62	0.38	4.33	0.92	2809
6.141	0.42681	17.66	1.86	0.23	4.84	1.14	2256
6.148	0.33947	17.79	1.69	0.30	4.40	0.95	2899
7.088	2.63760	16.73	1.54	0.51	4.03	0.85	2134

TABLE 1. (continued)

Name	$P(d)$	I	$V - I$	ΔI	M_I	$(V - I)_0$	d(pc)
7.096	0.44314	16.84	1.49	0.28	4.07	0.86	2337
7.103	0.29378	16.96	1.49	0.16	4.02	0.85	2492
7.107	0.32409	17.00	1.88	0.29	5.28	1.32	1501
7.133	0.45809	17.37	1.34	0.32	3.15	0.65	4301
7.134	0.38342	17.39	1.58	0.17	4.23	0.89	2604
7.143	0.37979	17.48	1.75	0.23	4.81	1.13	2261
7.144	0.67244	17.49	1.47	0.48	3.98	0.84	3282
7.148	0.47459	17.53	1.49	0.43	3.97	0.84	3271
7.150	0.32431	17.58	1.78	0.24	4.83	1.13	2290
7.161	0.46279	17.73	1.96	0.43	5.07	1.23	2005
7.165	0.90359	17.79	1.86	0.30	4.94	1.18	2329
8.055	1.57954	16.18	1.23	0.18	2.94	0.60	2865
8.074	0.24702	16.59	1.70	0.51	5.27	1.32	1409
8.110	1.09805	17.18	1.39	0.19	3.98	0.84	2979
8.114	1.20566	17.20	1.55	0.26	4.04	0.85	2686
8.118	0.59985	17.33	1.07	0.30	2.64	0.53	5946
8.121	0.91971	17.35	1.72	0.33	4.71	1.08	2206
8.129	0.34184	17.44	1.61	0.53	4.66	1.06	2442
8.131	1.53936	17.45	1.55	0.48	4.52	1.00	2648
8.136	0.38269	17.58	1.42	0.21	3.99	0.84	3482
8.145	1.73016	17.70	1.45	0.77	4.07	0.86	3515
8.150	0.41876	17.80	1.52	0.51	4.07	0.86	3554

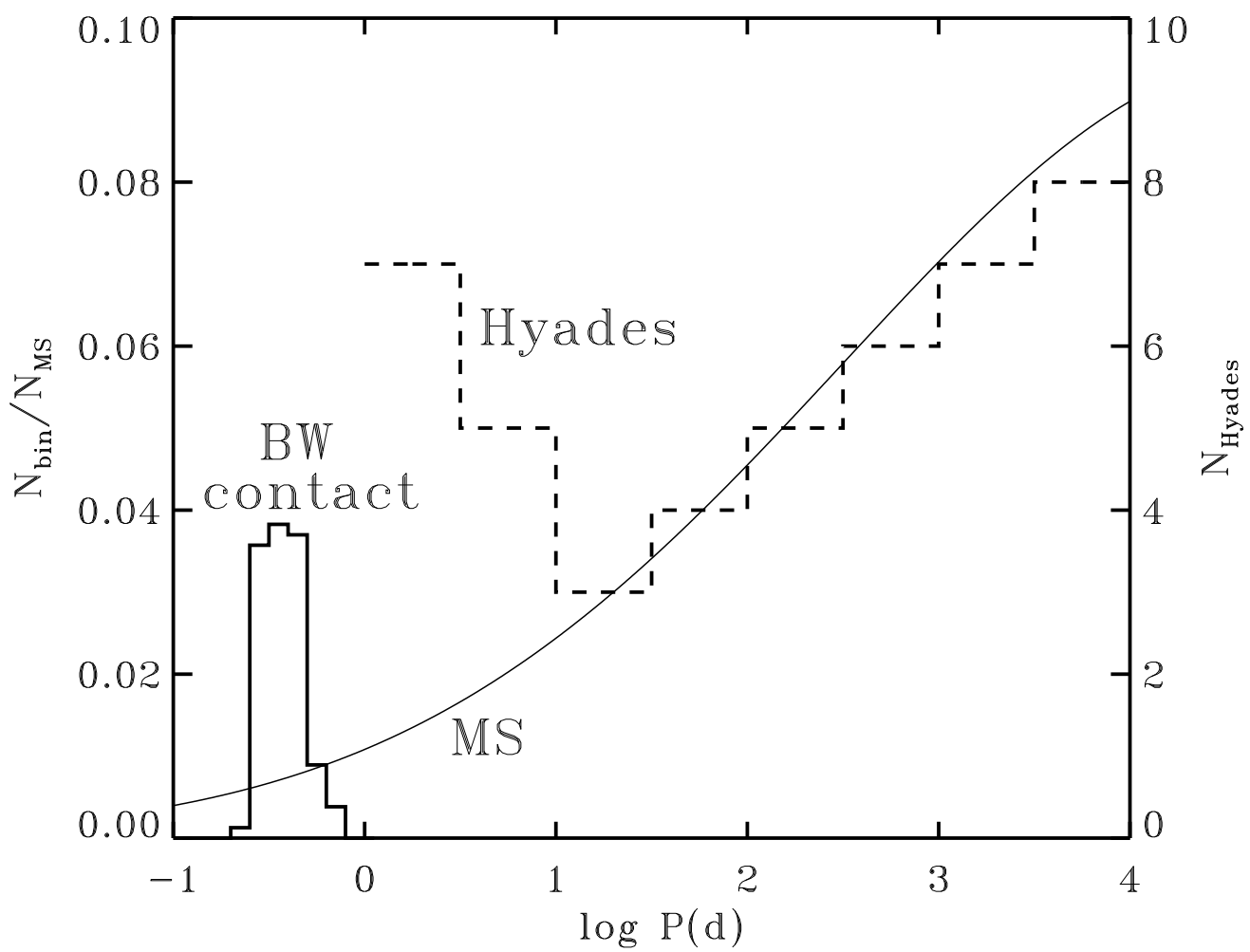


TABLE 1. Result of the statistical tests.

Test type	Samples	Results	
KS test	two equal size samples	$D_{KS} = 0.16$	$P_{KS} = 0.68$
KS test	FGK and M samples	$D_{KS} = 0.25$	$P_{KS} = 0.57$
$\log P - M_I$ corr.	full sample	$r_K = -0.003$	$r_S = -0.001$
$\log P - M_I$ corr.	FGK group	$r_K = 0.03$	$r_S = 0.04$
$\log P - (V - I)_0$ corr.	full sample	$r_K = -0.003$	$r_S = -0.002$
$\log P - (V - I)_0$ corr.	FGK group	$r_K = 0.03$	$r_S = 0.04$

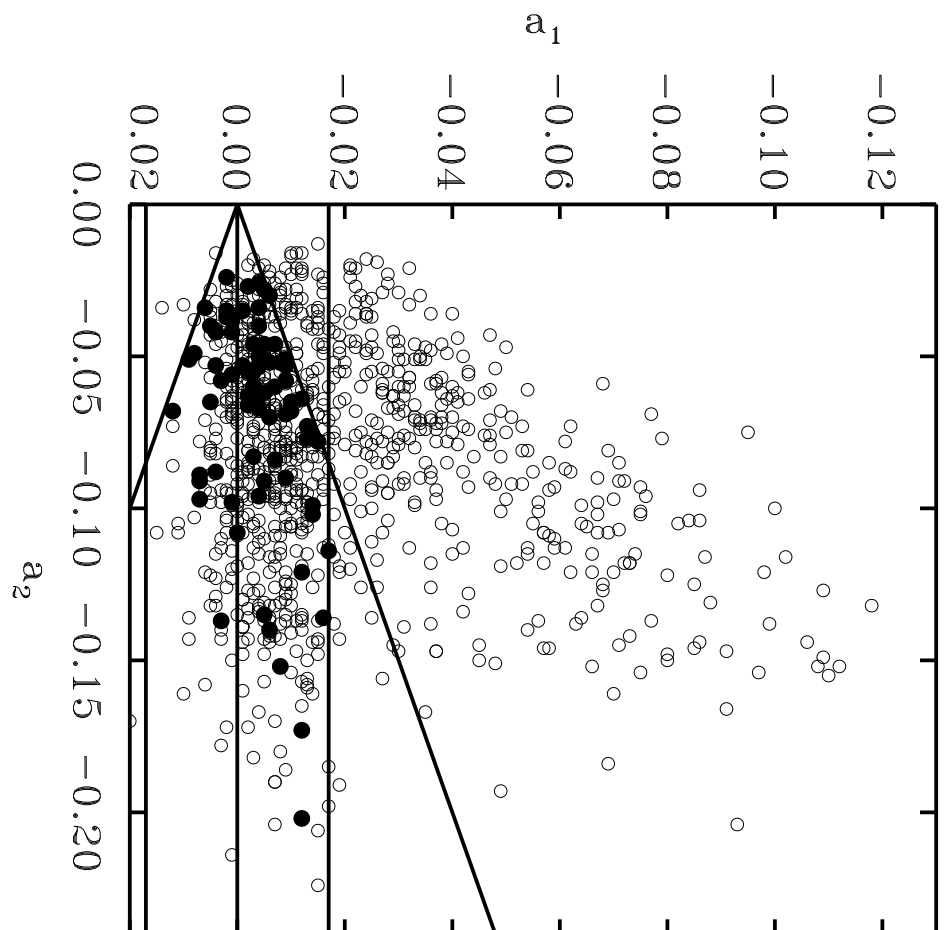
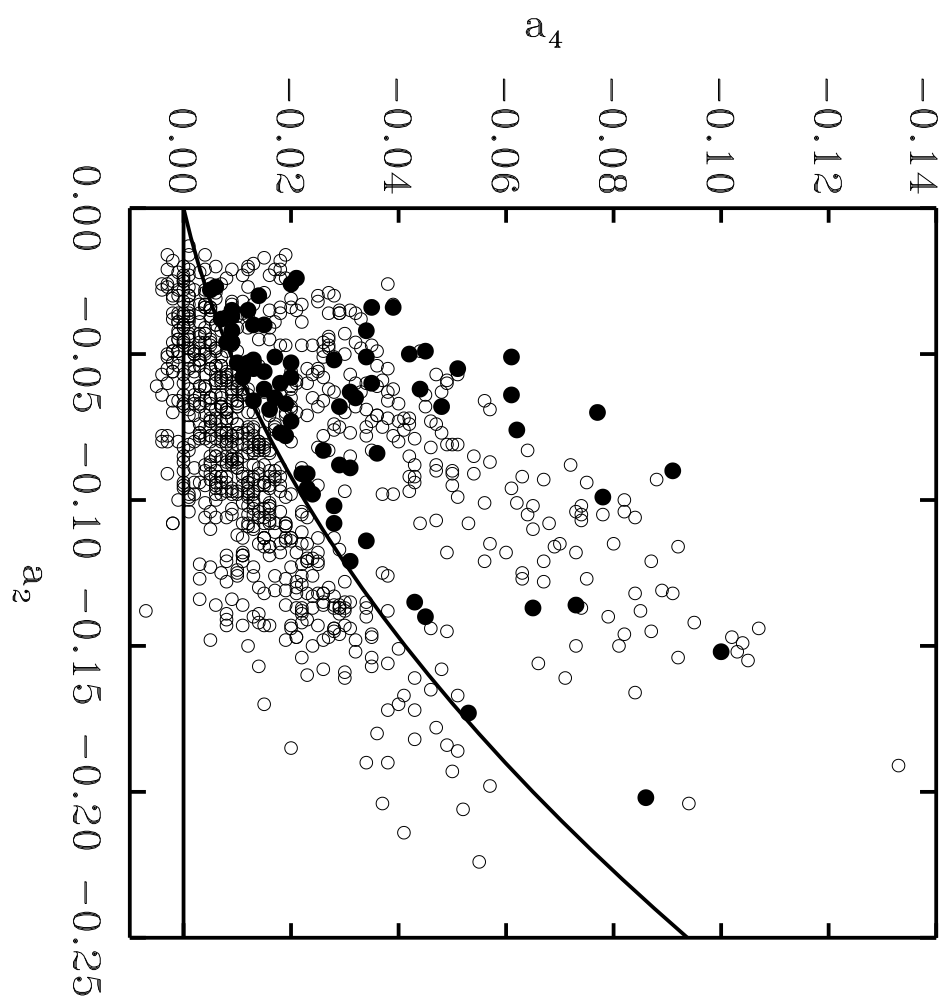


TABLE 1. Results of the Monte-Carlo determinations of coefficients A_0 and A_1 in
 $\log N = A_0 + a_1 \log P(\text{day})$

Term	median	1-sigma range	2-sigma range
Full			
A_0	1.07	-0.07, +0.05	-0.14, +0.11
A_1	-0.74	-0.18, +0.21	-0.40, +0.38
FGK			
A_0	1.03	-0.08, +0.06	-0.15, +0.11
A_1	-0.73	-0.22, +0.22	-0.43, +0.49

